Detecting failure of climate predictions

Michael C. Runge[1]★, **Julienne C. Stroeve**[2,3], **Andrew P. Barrett**[2] and **Eve McDonald-Madden**[4]

The practical consequences of climate change challenge society to formulate responses that are more suited to achieving long-term objectives, even if those responses have to be made in the face of uncertainty[1,2]. Such a decision-analytic focus uses the products of climate science as probabilistic predictions about the effects of management policies[3]. Here we present methods to detect when climate predictions are failing to capture the system dynamics. For a single model, we measure goodness of fit based on the empirical distribution function, and define failure when the distribution of observed values significantly diverges from the modelled distribution. For a set of models, the same statistic can be used to provide relative weights for the individual models, and we define failure when there is no linear weighting of the ensemble models that produces a satisfactory match to the observations. Early detection of failure of a set of predictions is important for improving model predictions and the decisions based on them. We show that these methods would have detected a range shift in northern pintail 20 years before it was actually discovered, and are increasingly giving more weight to those climate models that forecast a September ice-free Arctic by 2055.

Recognizing the decision context of climate change issues identifies a meaningful role for empirical science, and shifts the debate to pragmatic solutions[1,2,4]. The central role of traditional climate science in decision-making processes is to provide probabilistic predictions about outcomes of interest under various management strategies[3]. These predictions are, of course, made with uncertainty. The explicit articulation of this uncertainty is healthy, because it allows both risk analysis and adaptive management[4]. With risk analysis, individuals and society can examine the consequences of taking (or not taking) any action and being wrong, and so search for solutions that appropriately weigh the various risks. With adaptive management, management actions can be adjusted in response to new information that reduces uncertainty; indeed, the anticipation of this learning may influence initial actions. Both risk analysis and adaptive management require the articulation of uncertainty as a set of alternative predictions about the future. For climate forecasting, the set of coupled general circulation models (GCMs) and the various forcing scenarios provide the basis for alternative predictions about the outcomes of many potential management actions[5].

The ability to learn and make good management decisions within an adaptive framework will depend on whether the true system dynamics are contained within, bounded by, or close to the set of models that capture current uncertainty. Two types of surprise could undermine this ability: first, the truth might not be bounded by the model set, because of a failure to anticipate some important elements of the system; or second, the system might change in unanticipated ways that lead the true dynamics outside behaviour predicted by the model set. Both of these unanticipated outcomes can be considered 'unknown unknowns' or 'black swans'[6]. Adaptive

management includes an internal layer of learning ('single-loop learning'[7]) that allows discernment among the existing predictions as information accrues, and adaptation of future management actions to that new understanding. In addition, a second layer of learning is needed, which examines whether the system is responding as might be expected given the model set available, or if, instead, unpredicted responses are occurring. In the latter case, 'double-loop learning'[8] is triggered, in which the model set itself is re-examined, in an effort to develop new hypotheses that explain the surprising results. For example, satellite observations of Arctic sea-ice extent declined faster than forecast by the World Climate Research Programme Coupled Model Intercomparison Project Phase 3 (CMIP3) models, leading to hypotheses for the discrepancy and efforts to improve subsequent models[9]. The first step in double-loop learning is the detection of the failure of the model set. Early detection of failure of a set of predictions can trigger the process of diagnosis and the process of generating new predictions, quickly turning 'unknown unknowns' into 'known unknowns' and leading to better ongoing management and policy interventions through adaptive management.

In this paper, we develop methods for detecting the failure of a single model and the failure of a model set. We illustrate these methods in two contexts: detecting a shift in breeding distribution for northern pintails (*Anas acuta*)[10]; and detecting a failure of climate models to predict the loss of Arctic sea ice[9].

The role of models in a decision context is to make predictions about system response through time and as a function of management actions. These predictions are usually probabilistic[11], to represent uncertainty arising from a number of sources, including environmental variation, incomplete knowledge of system dynamics, sampling error, and incomplete control of management actions[12]. Thus, a model can be viewed as a hypothesis about the distribution of the response variable of interest. We would like our probabilistic predictions to be well calibrated and sharp[13]: over time, the observations should be compatible with the modelled distribution[14]. For example, in forecasting rainfall, we would like the observed frequency of wet and dry years to match the predicted (hindcast or forecast) frequencies generated by GCM simulations. The empirical distribution function (EDF) tests, a class of goodness-of-fit tests, examine the agreement between two continuous distributions using a statistic that measures the distance (D_n) between the empirical cumulative distribution from the real system ($F_n(x)$, where n is the accumulated sample size) and the cumulative distribution based on the prediction from the model ($F(x)$) (ref. 15). One of the advantages of the EDF tests is that the prediction can take any form of distribution. The Kolmogorov–Smirnov (K–S) test is one of many EDF tests, and uses the distance metric below.

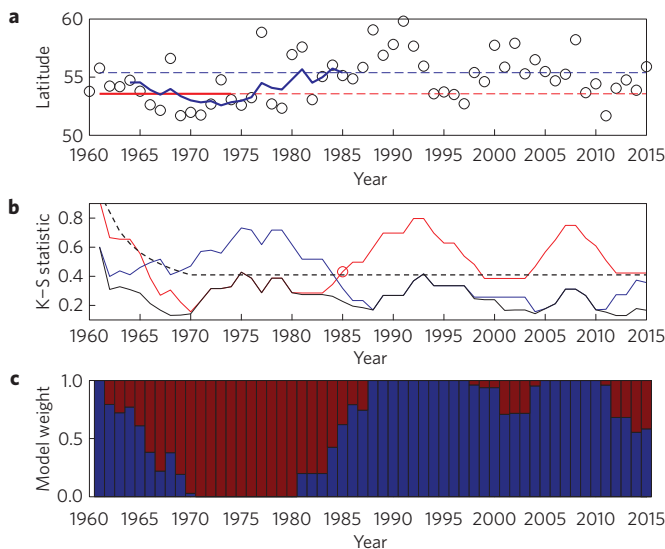$$D_n = \max_x |F_n(x) - F(x)| \qquad (1)$$

Figure 1 | Analysis of trends in distribution of northern pintails, 1961–2015.
a, Latitude of the centroid of the northern pintail (*A. acuta*) breeding
distribution. Model 1 (dashed red line) is the average for the period
1961–1974 (solid red line). Model 2 (blue line) is the five-year moving
average at 1985; the solid blue line shows the 5-year moving average for the
period 1965–1985. **b**, K–S fit statistics for Model 1 (red), Model 2 (dashed
blue line), and the best-weighted model (black), using a ten-year moving
window of the data. The nominal critical value ($\alpha = 0.05$) is shown as a
dashed line. The circle at 1985 shows the first point at which the K–S
statistic for Model 1 exceeded the critical value. **c**, Weights on Models 1
(red) and 2 (blue) that provide the best fit to a ten-year moving window of
observations, as measured by the K–S statistic.

The northern pintail is a waterfowl species that is important
for recreational hunting in North America[16]. Pintails depend on
ephemeral prairie wetlands for breeding and their dynamics are
strongly influenced by climatic conditions[17]. The annual distribu-
tion of this species, as measured by the latitude of its centroid, is
an indicator of the habitat conditions, with individuals breeding
farther north in drier years. As reproductive rate is also associated
with habitat condition, the latitude of the breeding population is
used as a predictor in setting hunting regulations[18]. Between 1961
and 1974 the mean latitude of the breeding distribution was 53.569
(s.d. = 1.549) (Fig. 1a, red line). Data collected from the mid-
eighties onwards shows a northerly shift in the pintail distribution,
but given the variability in the data it is difficult to discern if or when
this shift occurred and whether concerns should be raised about the
harvest rates set using Model 1. The K–S statistic shows that the
observations were compatible with Model 1 (Fig. 1b, red line) until
1985 (red circle). After 1985, the distance between the observations
and the predictions under Model 1 suggests a significant change in
the pintail distribution. In this way, an EDF statistic can be used to
identify when a single model is no longer plausible.

Often, a decision-maker will entertain several different expla-
nations of cause and effect in a system, that is, several alternative
models. These models may represent a comprehensive set, in the
sense that the truth is believed to be one of the models, but more
commonly, the hope is merely that the set of models somehow
bounds the truth. What would it mean for a model ensemble to
bound the truth? We propose this means there is weighted combi-
nation of the models in the set that makes predictions consistent
with the observations. If that is not the case, then the observations
are falling outside anything predicted by the ensemble, which would
indicate the need for careful evaluation of the model set. The EDF
statistic for the best-weighted model, then, is a measure of the
plausibility of the model set.

There are a number of ways that models could be weighted
to form an intermediate model. One possibility is to form a
linear-weighted average of the cumulative distribution functions
for each model. Another way is to average the moments of the
individual distributions. In either case, the best-fitting weighted
model minimizes the EDF statistic. In the examples that follow,
we have used the second weighting method, because we were
particularly interested in bounding the first two moments, but the
first weighting method may be appropriate in other contexts.

In 1985, when the observed pintail data indicated a divergence
from the 1961–1974 model (Model 1), a possible response would
have been to propose a second model with a fixed mean of 55.374
(the 5-yr moving average in 1985) and standard deviation of 1.549
(Fig. 1a, dashed blue line). This second model was not plausible
between 1970 and 1985 (as judged against a K–S test with nominal
$\alpha = 0.05$), but became plausible in 1985 and has remained so since
(Fig. 1b, blue line). The weights in the best-fitting weighted model
show the change in system dynamics (Fig. 1c): between 1971 and
1980, Model 1 received all of the weight; by 1988, all of the weight
had shifted to Model 2; and since 1998, the weights have fluctuated.
In the period 1988–1998, having all of the weight on Model 2 raises
the question of whether the true dynamics have moved outside the
model set and Model 2 is just the best approximation available.
Nevertheless, the best-fitting weighted model remains plausible over
the entire time series, suggesting that the two-model ensemble set
bounds the true range dynamics of the northern pintail at present
and would have performed well for setting harvest rates (Fig. 1b,
black line). Use of the Anderson–Darling statistic (another in the
class of EDF tests[15]) instead of the K–S statistic produces quite
similar results, with two minor differences: first, the failure of
Model 1 alone is detected in 1984 instead of 1985; and second, for
one year in 1993, the test warns that the model set may be failing.
(See Supplementary Information for a comparison of the power of
these two tests.)

The rapid loss of Arctic sea ice over the past two decades has
been one of the most visible and marked effects of global climate
change[19] and has led to significant concern about many aspects of
the Arctic environment, including, for example, the status of polar
bears[20,21]. Sea-ice extent and volume have been declining at a rate
that was faster than forecast by the CMIP3 models[9]. More recent
models (CMIP5) match the trends in the observed record better[22]
(Fig. 2a), but the question remains whether they are capturing the
Arctic sea-ice dynamics well enough to support decision-making.
The K–S statistics for the individual CMIP5 models (historical
and Representative Concentration Pathway (RCP)8.5 emissions) are
relatively stable from the early 1980s to the mid-1990s, but show
substantial shifts beginning about 1995 (Fig. 2b), with one model
that had previously fitted the observed time series well (CESM1)
falling out of favour, and several others beginning to show a better
fit (HadGEM2-CC, IPSL-CM5A-MR, MRI). Throughout this time
period, a linear weighting of the CMIP5 models can be found that
produces a satisfactory fit to the observations, suggesting that the
model set is still bounding the behaviour of the system (Fig. 2b, black
line). Nevertheless, the sharp changes in the individual K–S statistics
serve as an early indicator that the Arctic system is changing in a way
that is not captured by any one of the current CMIP5 models. If that
trend continues, the K–S statistic for the best-fit weighted model
may begin to indicate a failure of the entire model set, triggering
the need for new model development. This suggests that, for the
moment, the current set of models can be used by decision-makers
concerned about Arctic sea ice, but a watchful eye is needed to
be sure that the model set still bounds the observations over the
coming years.

As discussed above, the best-fit linear weighting of the CMIP5
models changed over time (Fig. 2c), particularly after 1995, when
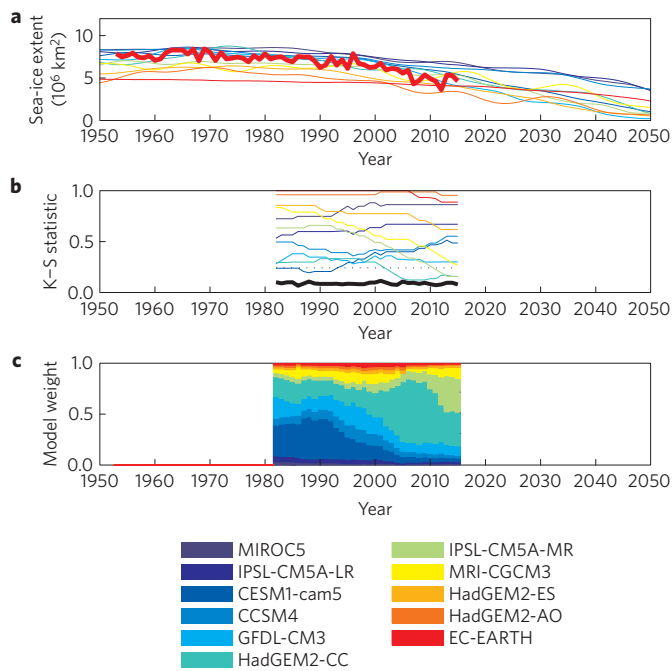the observed September sea-ice extent began to drop relative to the

Figure 2 | Analysis of trends in the extent of sea ice in the Arctic, 1953–2015. a, September Arctic sea-ice extent[22] (million km²). The thin lines show LOESS means from 11 CMIP5 models (RCP8.5). The thick red line shows the observed record. **b**, K–S fit statistics for the individual CMIP5 models and the best-weighted model (thick black line), using a 30-year moving window of the data. The critical value (nominal $\alpha = 0.05$) is shown as a dashed line. **c**, Weights on the individual CMIP5 models that provide the best fit to a 30-year moving window of observations, as measured by the K–S statistic.
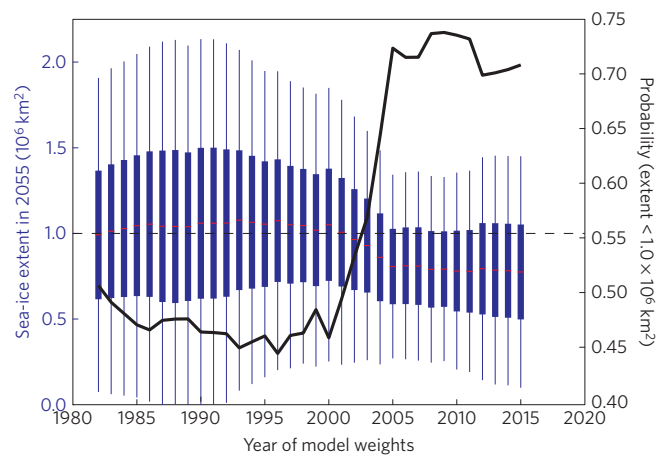
Figure 3 | Forecast extent of sea ice in the Arctic in 2055 as a function of the weights on the 11 CMIP5 models over the course of the observed record, and assuming the RCP8.5 forcing scenario. The boxplots show the 5%, 25%, 50%, 75% and 95% quantiles of the weighted model. The dashed line (at 1.0 million km²) is frequently cited as the threshold for an 'ice-free' Arctic. The black line shows the probability that the sea-ice extent will be less than 1.0 million km² in 2055, based on the best-fit weighted model.

multi-model ensemble of predictions. We can use these changing best-fit models over time to provide forecasts of the sea-ice extent in the future (Fig. 3), with the forecast changing as the model weights are updated with each year's observation. These results indicate that since 2000, the forecast September 2055 sea-ice extent under the RCP8.5 emission scenario has dropped; the most recent forecast (based on data through 2015) is 0.77 million km² (90% prediction interval: 0.10–1.45), very close to what is considered an 'ice-free' Arctic. This, in turn, has increased the probability that the sea-ice extent will be below 1.0 million km² from 44% using the model weights in 2000 to 71% using the model weights in 2015 (Fig. 3).

The model weights, the EDF statistics for the individual models, and the EDF statistic for the best-fitting weighted model provide a way to track system change and evaluate the multi-model ensemble. A shift in model weights over time may be an indicator that the dynamics of the system are changing (or that if the system dynamics are in fact stationary, such stationarity is not captured by the models in the ensemble). If the EDF statistic for the best-fitting weighted model remains plausible, then the multi-model ensemble is bounding the behaviour of the system. In contrast, if the EDF statistic for even the best-fitting weighted model is not plausible, then the ensemble is not functioning; a double-loop adaptation should be triggered, and the model set should be examined to try to explain the emerging surprises. In the case of northern pintails, this would have brought awareness to the change in system dynamics in 1985, twenty years before the effect was in fact identified and incorporated into management of hunting regulations. In the case of Arctic sea-ice extent, although the model set bounds the observed system behaviour at present, rapid shifts in the plausibility of individual models are an early warning that the current model set might be starting to fail.

Methods

Methods and any associated references are available in the online version of the paper.

References

1. McDonald-Madden, E., Runge, M. C., Martin, T. G. & Possingham, H. Optimal timing for managed relocation of species faced with climate change. *Nature Clim. Change* **1,** 261–265 (2011).
2. Conroy, M. J., Runge, M. C., Nichols, J. D., Stodola, K. W. & Cooper, R. J. Conservation in the face of climate change: the roles of alternative models, monitoring, and adaptation in confronting and reducing uncertainty. *Biol. Conserv.* **144,** 1204–1213 (2011).
3. Terando, A., Keller, K. & Easterling, W. E. Probabilistic projections of agro-climate indices in North America. *J. Geophys. Res.* **117,** D08115 (2012).
4. Lawler, J. J. *et al.* Resource management in a changing and uncertain climate. *Front. Ecol. Environ.* **8,** 35–43 (2010).
5. IPCC *Climate Change 2013: The Physical Science Basis* (Cambridge Univ. Press, 2013).
6. Taleb, N. N. *The Black Swan: The Impact of the Highly Improbable* (Random House, 2007).
7. Pahl-Wostl, C. A conceptual framework for analysing adaptive capacity and multi-level learning processes in resource governance regimes. *Glob. Environ. Change* **19,** 354–365 (2009).
8. Argyris, C. & Schön, D. A. *Organizational Learning: A Theory of Action Perspective* (Addison-Wesley, 1978).
9. Stroeve, J., Holland, M. M., Meier, W., Scambos, T. & Serreze, M. Arctic sea ice decline: faster than forecast. *Geophys. Res. Lett.* **34,** L09501 (2007).
10. Miller, M. R. & Duncan, D. C. The northern pintail in North America: status and conservation needs of a struggling population. *Wildl. Soc. Bull.* **27,** 788–800 (1999).
11. Dawid, A. P. Statistical theory: the prequential approach. *J. R. Stat. Soc. A* **147,** 278–292 (1984).
12. Williams, B. K., Johnson, F. A. & Wilkins, K. Uncertainty and the adaptive management of waterfowl harvests. *J. Wildl. Manage.* **60,** 223–232 (1996).
13. Gneiting, T., Balabdaoui, F. & Raftery, A. E. Probabilistic forecasts, calibration and sharpness. *J. R. Stat. Soc. B* **69,** 243–268 (2007).
14. Seillier-Moiseiwitsch, F. & Dawid, A. P. On testing the validity of sequential probability forecasts. *J. Am. Statist. Assoc.* **88,** 355–359 (1993).
15. Stephens, M. A. in *Goodness-of-fit Techniques* Vol. 68 (eds D'Agostino, R. B. & Stephens, M. A.) Ch. 4, 97–193 (Marcel Dukker, 1986).
16. Austin, J. E. & Miller, M. R. in *The Birds of North America* (ed. Poole, A.) (Cornell Laboratory of Ornithology, 1995).

17. Hestbeck, J. B. Response of northern pintail breeding populations to drought, 1961–92. *J. Wildl. Manage.* **59,** 9–15 (1995).
18. US Fish and Wildlife Service *Adaptive Harvest Management: 2014 Hunting Season* (United States Department of Interior, 2014).
19. Stroeve, J. *et al*. The Arctic's rapidly shrinking sea ice cover: a research synthesis. *Climatic Change* **110,** 1005–1027 (2012).
20. Amstrup, S. C. *et al*. Greenhouse gas mitigation can reduce sea-ice loss and increase polar bear persistence. *Nature* **468,** 955–958 (2010).
21. Hunter, C. M. *et al*. Climate change threatens polar bear populations: a stochastic demographic analysis. *Ecology* **91,** 2883–2897 (2010).
22. Stroeve, J. C. *et al*. Trends in Arctic sea ice extent from CMIP5, CMIP3 and observations. *Geophys. Res. Lett.* **39,** L16502 (2012).

Author contributions

M.C.R. and E.M.-M. conceived of the methods; J.C.S. and A.P.B. extracted the sea-ice forecasts from the CMIP5 models; M.C.R. analysed the pintail and sea-ice data and prepared the figures; and M.C.R., E.M.-M. and J.C.S. co-wrote the paper.

Additional information

Supplementary information is available in the online version of the paper. Reprints and permissions information is available online at www.nature.com/reprints. Correspondence and requests for materials should be addressed to M.C.R.

Competing financial interests

The authors declare no competing financial interests.

Methods

Data and models. For northern pintails, the data are the observed latitude of the breeding population in North America, 1961–2015, taken from the Waterfowl Breeding Population and Habitat Survey. Two models, both normally distributed, were compared: Model 1 predicted a constant mean and variance (based on the mean and variance of the observed latitude, 1961–1974); Model 2 used the five-year moving average at 1985 as the mean, and the same variance as Model 1. Both Models 1 and 2 use a fixed long-term mean, rather than a more complicated time-series model because harvest regulations for northern pintails are set assuming a fixed long-term mean for the latitude of the breeding population.

The sea-ice data measure the extent of sea ice in September (million km^2). The observational record is based on a combination of passive microwave sea-ice concentrations from the NASA Team sea-ice algorithm[23] and earlier satellite, aircraft and ship observations available from the Had1SST data set[24] that were merged to create a consistent time series[25]. Hindcast and forecast September sea-ice extent was extracted from 11 CMIP5 models (CCSM4, six ensemble members; CESM1-cam5, 3; EC-EARTH, 12; GFDL-CM3, 1; HadGEM2-AO, 1; HadGEM2-CC, 1; HadGEM2-ES, 4; IPSL-CM5A-LR, 4; IPSL-CM5A-MR, 1; MIROC5, 2; MRI-CGCM3, 1), using the RCP8.5 forcing scenario. The CMIP5 models use observed greenhouse gas concentrations through 2005 and forecast concentrations thereafter. The subset of 11 was chosen from the full set of CMIP5 models on the basis of their ability to capture basic features of the Arctic climate, as reflected in observed ice thickness distributions[26].

The CMIP5 model results are replicate simulations taking into account temporal variation, parametric uncertainty, and uncertainty in starting conditions; each replicate is a possible future trajectory. These results, however, are not in themselves probabilistic forecasts of sea-ice extent. To develop probabilistic forecasts of sea-ice extent, we used the replicate CMIP5 results to estimate time-specific means and variances. For each of the CMIP5 models, a year-specific mean was estimated with LOESS smoothing ($\lambda = 2$, 25-yr window for α), and a corresponding year-specific variance was estimated with LOESS smoothing of the variance of the residuals. The year-specific forecast was a normal distribution with the corresponding mean and variance. This method for developing probabilistic forecasts from the CMIP5 model results, including the assumption of a normal distribution, is one possible approach and seems to work well for the sea-ice metric; other approaches and distributions have been explored[3] and may be more appropriate for other metrics.

Individual model fit. To assess the fit of each model to the data, a moving window was used (ten years for the pintail data, 30 years for the sea-ice data). Within the moving window, the observations were expressed as a normalized residual from the corresponding year-specific predicted distribution. An empirical cumulative distribution function was formed from the set of residuals within the window and compared against the cumulative distribution function for a standard normal distribution to calculate the K–S statistic (equation (1)) or Anderson–Darling

statistic, with an appropriate critical value[15]. In a decision context, the choice of the critical value is an important value judgment that reflects the relative importance of Type 1 and Type 2 errors, and the nominal critical value needs to be adjusted to account for multiple comparisons as well as the estimation of parameters[27]. These topics are investigated in detail in the Supplementary Information. Throughout the main body of the paper, we have used the critical value associated with a nominal Type 1 error rate (α) of 0.05.

Weighted models. Weighted models were formed from the component models with linear weighting of the first two moments. For example, to combine the 11 sea-ice models, a set of 11 weights (summing to 1) were used to weight the 11 means and the 11 standard deviations. A set of weights were evaluated by calculating the K–S statistic for the weighted model in the preceding window associated with a particular point in time. The best-fit weighted model at each point in time was found by searching for the set of weights that minimized the K–S statistic: for the pintail example using multivariate constrained optimization, specifically, sequential quadratic programming[28]; for the sea-ice example using multivariate unconstrained optimization, specifically, a gradient-based quasi-Newton method[29] with a cubic line search procedure[28].

The sea-ice forecast based on a weighted model (Fig. 3) used the year-specific means and variances from the 11 CMIP5 models, weighted by the best-fit set of weights. Each of the 11 models has a forecast for the sea-ice extent in September 2055; these forecasts were weighted by the sets of weights at each point in the observational record. The quantiles were found by assuming that the weighted forecast was normally distributed.

References

23. Cavalieri, D. J., Parkinson, C. L., Gloersen, P. & Zwally, H. J. *Sea Ice Concentrations from Nimbus-7 SMMR and DMSP SSM/I-SSMIS Passive Microwave Data* (NASA DAAC at the National Snow and Ice Data Center, 1996).

24. Rayner, N. A. *et al.* Global analyses of sea surface temperature, sea ice, and night marine air temperature since the late nineteenth century. *J. Geophys. Res.* **108,** 4407 (2003).

25. Meier, W. N., Stroeve, J. & Fetterer, F. Whither Arctic sea ice? A clear signal of decline regionally, seasonally and extending beyond the satellite record. *Ann. Glaciol.* **46,** 428–434 (2007).

26. Stroeve, J., Barrett, A., Serreze, M. & Schweiger, A. Using records from submarine, aircraft and satellites to evaluate climate model simulations of Arctic sea ice thickness. *Cryosphere* **8,** 1839–1854 (2014).

27. Babu, G. J. & Rao, C. R. Goodness-of-fit tests when parameters are estimated. *Sankhyā: Indian J. Stat.* **66,** 63–74 (2004).

28. Fletcher, R. *Practical Methods of Optimization* (John Wiley, 1987).

29. Shanno, D. F. Conditioning of quasi-Newton methods for function minimization. *Math. Comput.* **24,** 647–656 (1970).